

Development of a Novel Rivet-Based Joining-by-Forming Process Using Flat Dies

Unni Daniel Yeniss^{1,a*} and Strano Matteo^{1,b}

¹Politecnico di Milano, Mechanical Engineering Dept., Via La Masa, 1, Milan, 20156 Italy

^{a*}danielyeniss.unni@polimi.it, ^bmatteo.strano@polimi.it

*corresponding author

Keywords: joining by forming, rivet design, sheet metal joining, cold joining, low cost tooling, end of life (EoL) vehicles, sustainable manufacturing

Abstract. The direct reuse of End-of-Life (EoL) automotive sheet metal offers significant environmental benefits, particularly when panels are flattened rather than remelted. However, the geometric irregularity and variable formability of reclaimed sheets require joining solutions that operate with minimal tooling and are compatible with flat-die pressing. This work introduces a novel rivet-based joining-by-forming process designed to create a mechanical interlock using only flat tools, enabling integration into the same hydraulic press used for EoL panel flattening. Finite element simulations were performed to optimize rivet geometry and study flange formation, stress distribution, and failure mechanisms. The optimized rivet design achieves stable outward flaring under axial compression, producing a functional joint without shaped dies. Experimental tests on reclaimed automotive sheets validated the joining concept and confirmed the deformation behaviour predicted numerically. The proposed method provides a low-cost, low-energy joining strategy suitable for reclaimed steels of uncertain formability and supports the development of circular manufacturing routes based on the direct reuse of automotive sheet metal.

Introduction

The transition toward low-carbon industrial systems requires the adoption of new sustainability strategies in sectors characterized by high material and energy intensity. Transportation alone accounts for approximately 25% of global energy consumption [1] and 21.9% of world steel demand [2], with the automotive industry responsible for 19.8% of the total steel used annually [2]. In a typical 1481 kg passenger vehicle, steel constitutes nearly half of the total mass, approximately 47%, highlighting the critical role of metal use in this sector [3]. In this context, improving the resource efficiency of automotive metals represents a high-impact opportunity for advancing Circular Economy objectives beyond conventional recycling.

Farioli et al. [4] recently introduced an alternative recovery strategy for End-of-Life (EoL) automotive panels that avoids energy-intensive remelting. Their approach reshapes curved automotive body components into flat sheet metal through a controlled flattening operation using a hydraulic press. The overall recovery workflow consists of four primary stages (Fig. 1):

- (1) selection of EoL vehicle body panels;
- (2) material extraction through cutting and disassembly;
- (3) flattening of the curved panels into planar sheets;
- (4) paint removal using mechanical, chemical, or laser-assisted methods.

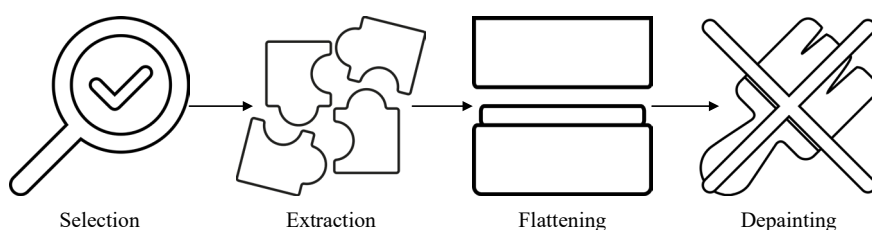


Fig. 1. Scheme of the EoL sheet metal recovery process.

This process offers substantial environmental benefits compared to recycling. For each kilogram of steel recovered through flattening, approximately 2.2 kg of CO₂ emissions and 24 MJ of energy can be saved [4]. Additional evidence from Ali et al. [5] shows that direct reuse of scrap sheet metal within manufacturing can reduce costs by 40% and energy consumption by 67%. They demonstrated that irregularly shaped automotive scrap sheets can be directly reused by employing a Voronoi-based geometric algorithm to generate façade panels from heterogeneous offcuts. Since the scrap pieces differ significantly in shape and size, the Voronoi tessellation allows the target surface to be subdivided into polygons that can be efficiently matched to the available sheets, minimizing trimming waste and avoiding remelting.

This example highlights a crucial constraint of upcycling workflows: reclaimed sheets must often be combined to obtain larger functional components, making an efficient, low-tooling joining method essential.

The geometrical and material variability of End-of-Life (EoL) automotive panels introduces significant technical challenges for their direct reuse. Recovered sheets typically exhibit heterogeneous dimensions, variable thickness, pre-existing damage, surface degradation, and reduced or uncertain formability due to ageing and prior deformation history. Consequently, the reuse of flattened EoL sheet metal requires a rethinking of downstream manufacturing operations. In particular, the intrinsically limited size of individual body panels makes joining operations essential to produce larger sheets or structural subassemblies suitable for secondary applications.

Available joining-by-forming technologies such as clinching, self-piercing riveting (SPR), and double-sided SPR are widely recognized for providing reliable mechanical joints with comparatively low environmental impact relative to fusion welding [6, 7]. However, these processes rely on shaped dies, controlled material ductility, and dedicated tooling. Such requirements are difficult to satisfy when working with reclaimed automotive sheet metal characterized by thickness variability, unknown forming history, and degraded or uncertain ductility. Blind riveting appears to be a suitable solution, but it suffers from intrinsic drawbacks, including low process speed and the formation of protrusions incompatible with functional or aesthetic surface requirements. More generally, existing rivet-based solutions mostly require pre-formed features, contoured dies, or proprietary equipment, which limits their integration into flexible, low-cost reuse workflows.

Novelty of the present Work.

The contribution of this study is a rivet-based joining-by-forming concept explicitly engineered for flattened End-of-Life (EoL) automotive sheets, where thickness, surface condition, and ductility are often uncertain and where the available equipment is typically a flat-tool hydraulic press used for panel flattening. Unlike clinching and self-piercing riveting, which rely on shaped die cavities and controlled sheet flow, the proposed joint is generated with two flat dies: a purposely profiled rivet stem is axially compressed to trigger a repeatable outward buckling mode, forming a circumferential flange that mechanically locks the sheet stack. The rivet geometry (chamfer, stem length, and head–shank radius) is designed to (i) stabilize the buckling path, (ii) promote outward flaring rather than inward collapse, and (iii) tolerate high pressing forces without dedicated tooling. This enables the joining operation to be performed in the same press and with the same flat tooling already used for EoL panel flattening, reducing capital cost and simplifying integration into reuse workflows. To the authors' knowledge, this is the first rivet-based joining-by-forming approach demonstrated to create a functional mechanical interlock under flat-die conditions and validated numerically and experimentally on reclaimed automotive sheet metal.

In Fig. 2, two examples are shown of upcycled components produced from reclaimed automotive panels, demonstrating how geometrically limited and irregular sheets can nonetheless be transformed into high-value products, underscoring the need for efficient joining solutions to enable such applications.



Fig. 2. Examples of products obtained from upcycled automotive sheet metal. From left to right, Tables obtained from scrapped automotive sheets, made by Weld House (Photo by Dornob). A table obtained from an Opel Admiral car, made by Unibro Design.

Designed Rivet Working Principle

The proposed joining concept is designed to operate using only a flat punch and flat die, identical to the tools already employed in the EoL sheet-flattening process. This allows the joining operation to be seamlessly integrated into the same hydraulic pressing workflow without additional tooling. The joint is formed through a sequence of deformation stages in which a specially designed rivet undergoes controlled buckling and flange formation to create a mechanical interlock between the sheets.

The process begins with the insertion of the rivet into two pre-drilled holes in the sheet stack, with a clearance of 0.1 mm between the rivet shank and the hole diameter (Fig. 3a). The rivet head is positioned on the die side, while the stem faces the punch. As the punch advances, the rivet stem is compressed axially and undergoes progressive buckling, causing the lower portion of the stem to flare outward and form an expanding flange (Fig. 3b). Concurrently, the sheets are forced into contact with the underside of the rivet head, and slight upward bending of the upper sheet may occur as the stack accommodates the developing flange (Fig. 3c).

Continued punch displacement forces the flanged region into a fully flattened configuration, securing the sheets between the rivet head and the newly formed flange (Fig. 3d). The resulting interlock is generated entirely through plastic deformation of the rivet stem and the localized bending of the sheets, without relying on a shaped die cavity. This characteristic differentiates the proposed solution from conventional riveting, clinching, and self-piercing riveting processes, and enables a low-cost joining operation compatible with reclaimed sheet metal of variable formability.

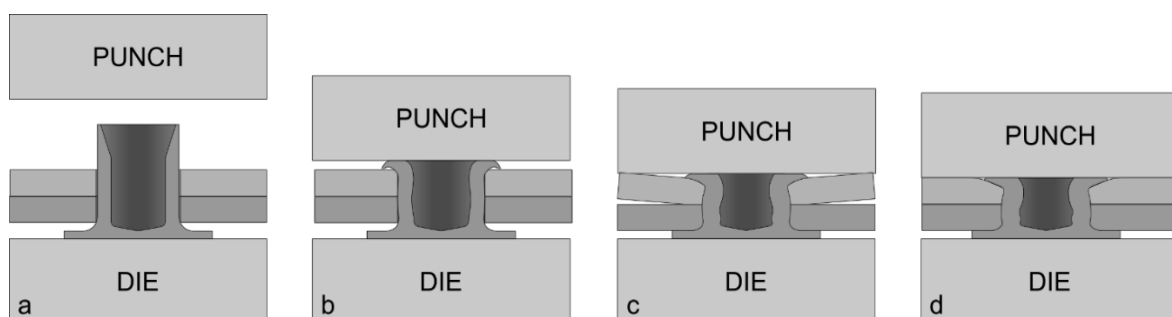


Fig. 3. Representation of the proposed rivet joining method using flat tools.

Numerical and experimental investigations (described in the following sections) demonstrate that rivet geometry, particularly the chamfer length, head-shank radius, and stem length plays a decisive role in controlling the buckling mode, flange extent, and final interlock quality. The deformation path must be carefully tuned to ensure outward flaring rather than uncontrolled buckling, while minimizing excessive sheet displacement or surface irregularities.

Both numerical simulations, using Transvalor Forge, and experimental tests, with a Pezzato CB AUTO hydraulic press machine, have been performed on the novel rivet design. Experimental tensile tests have been performed with an MTS Alliance RT/100 machine. Both numerical simulations and experimental tests were conducted using DC04 low carbon steel sheets (Table 1). Stainless Steel 303, sourced from the Xometry materials catalog, was selected as the rivet material. For the experimental phase, rivet prototypes were CNC machined from this material.

Table 1. Materials used in the tests. DC04 steel characteristics are based on Trzepieciński and Najm work [8].

Materials used in the numerical simulations			
Grade	Yield Stress [Mpa]	Tensile Strength [Mpa]	Elongation [%]
Stainless Steel 303	351	398	31
DC04 Steel	210	270 - 350	38

Numerical Simulations

Finite element simulations were conducted using Transvalor Forge to evaluate the deformation behavior of the proposed rivet geometry and to investigate flange formation, sheet displacement, and failure tendencies under flat-die compression. All simulations employed 1 mm thick DC04 steel sheets and were performed with a pressing strength of 25 tons. The rivet material was modeled using stainless steel 303 properties, as reported in Table 2.

Due to the axisymmetric nature of the initial rivet deformation process, most simulations were performed in a 2D axisymmetric configuration, enabling reduced computational cost while accurately capturing the buckling and flanging behavior of the rivet stem. The punch and die were modeled as rigid bodies, whereas the rivet and sheets were modeled as elasto-plastic deformable solids.

Material behavior was described using an isotropic hardening law, calibrated from tensile tests for the reclaimed DC04 sheets and literature data for the AISI 303. A Coulomb-limited Tresca friction model was applied at all contact interfaces, using a Coulomb friction coefficient of 0.05 and a Tresca shear factor of 0.1, to represent a low-friction metal-to-metal interaction. The Coulomb value ($\mu = 0.05$) is commonly adopted in sheet-metal forming to model low friction, while the Tresca parameter ($m = 0.1$) was set in accordance with the software guidelines, which recommend using a Tresca value approximately twice the Coulomb coefficient. Although the selected coefficients provide a reasonable and stable baseline for the present study, a dedicated sensitivity analysis is currently underway to select the optimal friction coefficients. The adopted values should be regarded as starting minimal friction coefficients. Mesh refinement was applied in regions of high expected strain gradients, with a minimum 2D element size of approximately 0.1 mm, ensuring accurate capture of the buckling mode and localized thinning. Typical computation times ranged from approximately 30 to 50 minutes for 2D simulations to more than 5 hours for full 3D models. Numerical simulations were validated by visually comparing the simulations results and the pressed rivet in the experimental phase, which will be discussed more in detail later in this work.

The rivet geometry (Fig. 4) is inspired by commercially available self-piercing rivets and incorporates the following distinctive features:

- A 4.0 mm stem length and 3.3 mm diameter, ensuring sufficient material flow and outward flaring under compression to create a stable mechanical interlock.
- An extended, sharpened chamfer designed to minimize the contact area between the flat surface at the end of the chamfer and the hydraulic press punch. This geometry enables earlier

contact between the punch and the chamfer, thereby reducing the risk of inward buckling, which would lead to joint failure, and promoting controlled outward flaring necessary for joint formation.

- A reduced fillet radius between the underside of the rivet head and the base of the stem, maximizing the contact area between the rivet and the sheet metal during pressing and enhancing load transfer within the joint.

The rivet when pressed, correctly flanged outwards leading to the creation of a constraint in the punch side and on the die side thanks to the sheets being pushed against the head, granting further resistance to the joint (Fig. 5).

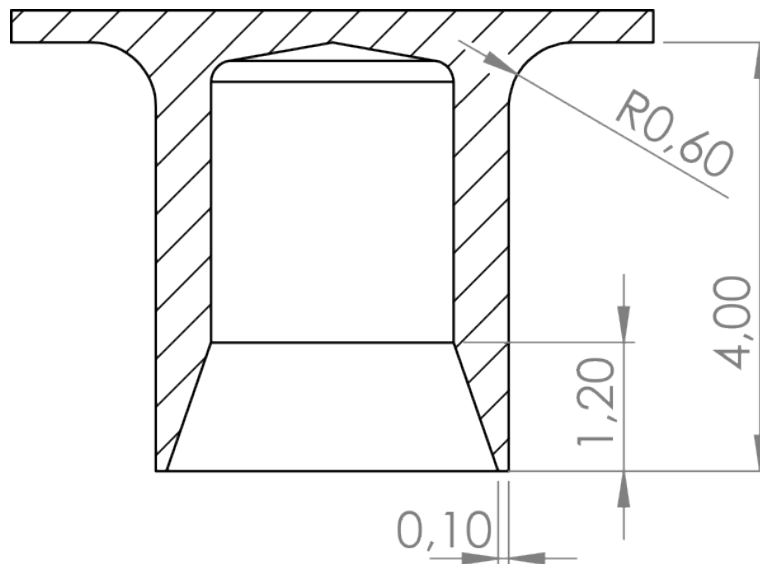


Fig. 4. Section view of the new version of the rivet.

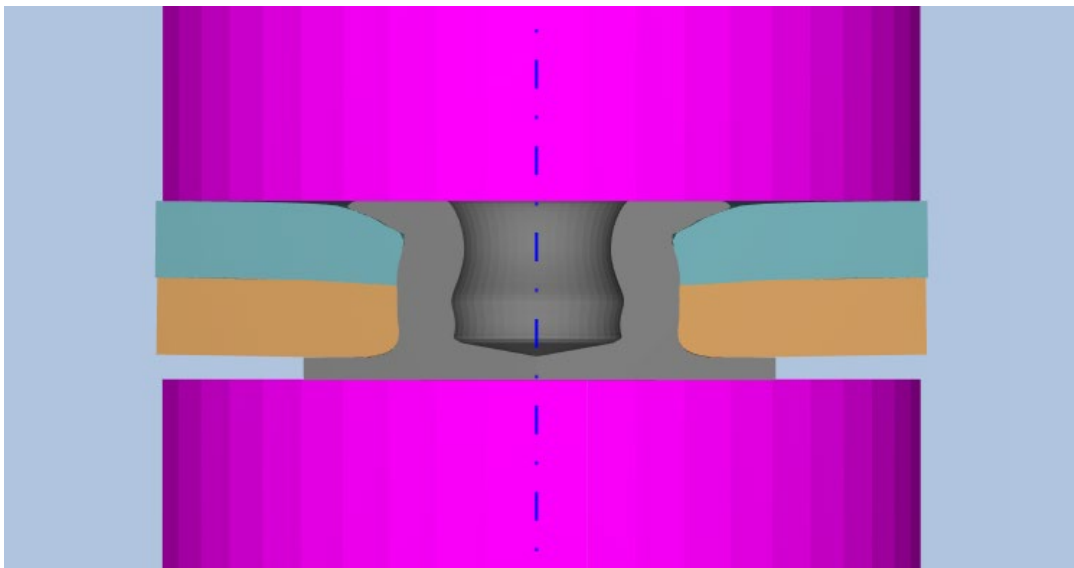


Fig. 5. Result of the numerical simulation on the third tested rivet. A working connection is formed.

The numerical simulations allowed to see the Latham Cockroft normalized criterion on the pressed rivet and assess its damage mode when the joint is being created. Both in the initial setup and reversed orientation, the rivet showed high stresses and fractures around the border of the flared stem (Fig. 6), leading to cracks that are radially distributed similar to an asterisk. Numerical simulations showed that in the rivet with the head lying on the die side, like in fig. 3, presented deeper but more localized fractures (Fig. 6a); whereas the rivet in reversed orientation, with the head pointing towards the punch side, showed less deep but more numerous fractures leading to a less defined and more wavy border of the pressed stem, compared to the rivet pressed in with the head pointing towards the die side (Fig.

6b). A reason of this difference in behaviour can be found in the fact that the rivet when pressed in its reversed orientation, has its stem inserted through the pre-drilled holes and the material flow when pressed is constrained by the material of the parts to join, whereas the rivet when pressed with the head pointing towards the die side has the stem bulging out of the pre-drilled hole and finds less constraints in its flow when pressed.

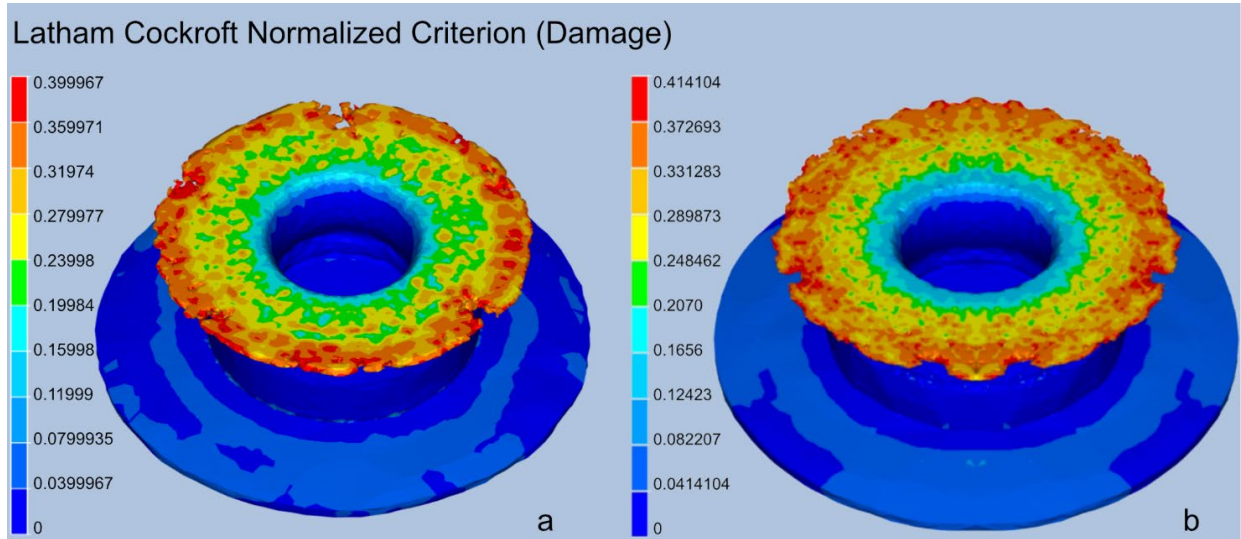


Fig. 6. Latham Cockcroft normalized Criterion of the pressed rivet (a) and of the pressed rivet with reversed orientation (b). The simulation on the reversed rivet (b) is symmetrical and was performed only on one half of the model.

To estimate joint strength, push-out simulations were performed in which a punch applied force through the hollow rivet core while the sheets were clamped between blankholders (Fig. 7). Pushout simulations showed an estimated maximum force of the joint of 2.503 kN.

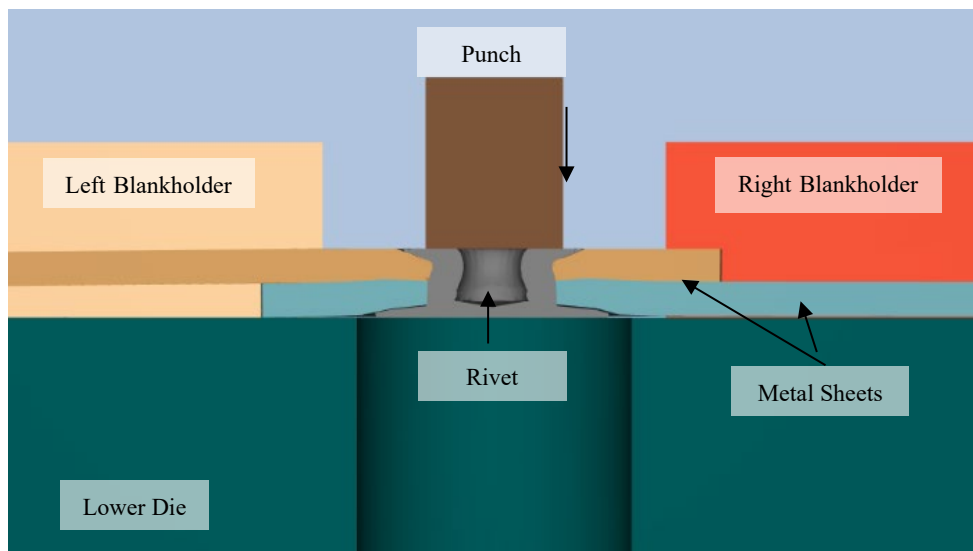


Fig. 7. Setup of the pushout simulations. Red and yellow are the blankholders, the punch is the brown element. The dark green lower die has a hole to allow the falling of the pushed out rivet.

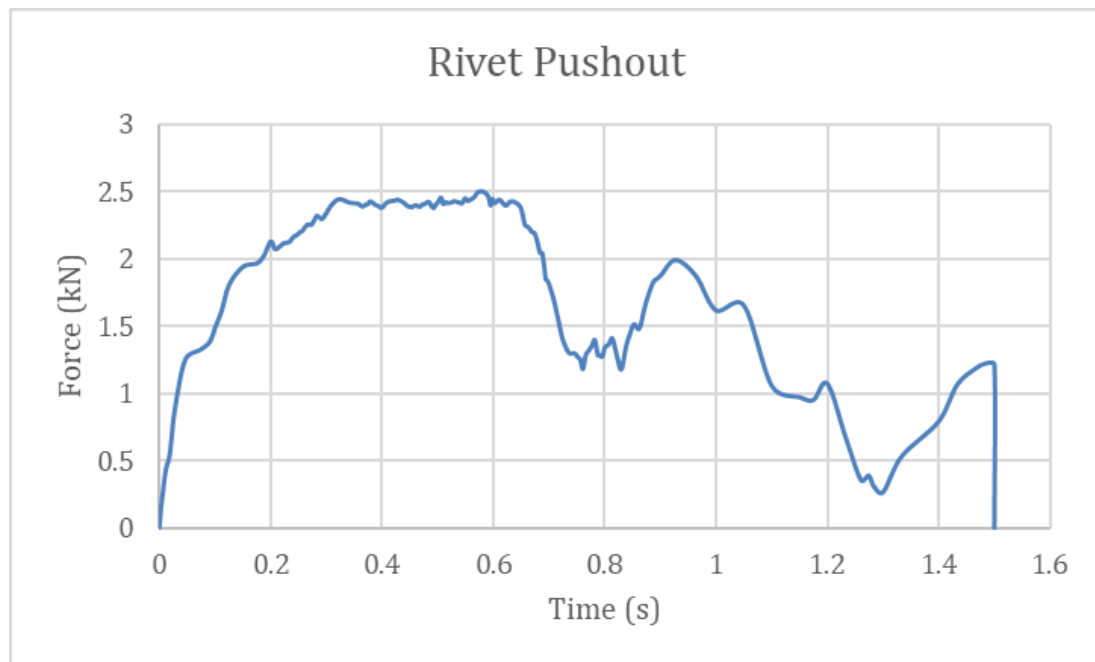


Fig. 8. Plots of the required force vs. pressing time in the pushout numerical simulations.

Experimental Riveting Tests

Experimental tests were conducted to validate the feasibility of the rivet-based joining process and to compare the deformation behavior observed in simulations with real pressed samples. Prototypes of the optimized rivet were CNC-machined from AISI 303 stainless steel, matching the geometry and material properties used in the numerical models. All experiments were performed using a Pezzato CB AUTO hydraulic press, equipped with flat punch and die surfaces identical to those used for the EoL sheet-flattening process and set on 25 tons pressing force.

Automotive sheet-metal offcuts recovered from hoods and roofs were selected as representative EoL materials, and a sample of 0.99 mm thickness was selected, comparable to the 1.0 mm used in the FEM simulations, enabling direct comparison between numerical and experimental results. Each dogbone specimen was cut at mid-length, and a single 3.5 mm diameter hole was drilled 6.5 mm from the cut edge. The rivet was inserted into this hole before pressing.

During pressing, the rivet stem underwent significant plastic deformation, forming the outward flange responsible for the mechanical interlock. In both orientations, fractures developed along the deformed stem, consistent with high strain localization predicted by simulations.

Fig. 9 illustrates representative pressed rivets used to join samples obtained from EoL automotive sheet metal. The rivet flared outward to form a retaining flange. The upper sheet exhibited slight upward bending, in agreement with simulation predictions. No fractures were observed in the sheet metal itself. The pressed rivet on the left hand side of the picture was pressed with the rivet head lying on the die side and the stem pointing towards the punch, whereas the right hand side joint presents the rivet reversed with the head pointing towards the punch side. In both cases the rivets formed reliable interlocks and confirm that the geometry is robust and that flange formation is reliably achieved using flat dies, without requiring any contoured or specialized tooling. The fractures starting from the borders of the rivet and disposed circularly were expected from the numerical simulations results and are caused by the high pressing force. The fractures around the rivets are caused by the pressing force and affect only the paint layer over the EoL sheet metal from the samples, the sheets material was not damaged.

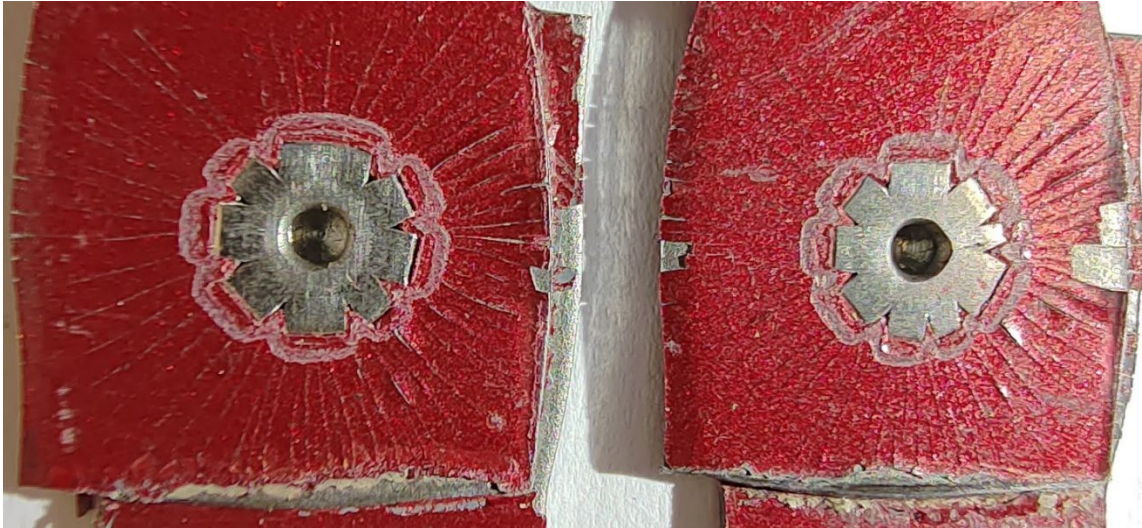


Fig. 9. On the left hand side the pressed rivet with the initial setup orientation, on the right hand side the rivet pressed in the reversed direction with the head on the punch side.

16 tensile tests were performed on the pressed samples using a MTS Alliance RT/100 universal testing machine. Both single rivets and double rivets setups were tested in both orientations, as shown in Fig. 3 and with the setup reversed, where rivet head points towards the punch side. The reversed rivets showed a slightly lower load-bearing capacity.

Table 2. Maximum loads of the tensile tests of single rivet setups. (r) indicates a rivet pressed with reversed orientation.

Single Rivet Setup				
Thickness (mm)	Test 1 (kN)	Test 2 (kN)	Test 3 (kN)	Average (kN)
0.75	1.17	1.499	1.174	1.281
0.83	1.297	1.449	1.245 (r)	1.33
0.99	1.785	1.624	1.722 (r)	1.71

Table 3. Maximum loads of the tensile tests of double rivet setups. (r) indicates a rivet pressed with reversed orientation.

Double Rivet Setup				
Thickness (mm)	Test 1 (kN)	Test 2 (kN)	Test 3 (kN)	Average (kN)
0.75	2.306	2.12	-	2.213
0.83	2.704	2.646	-	2.675
0.99	2.464	2.552	2.557 (r)	2.524

Validation of Numerical Simulations.

The numerical model was validated by comparison with experimental observations in terms of deformation mode and damage localization. The simulations predict a progressive axial compression of the rivet stem followed by a controlled outward buckling and flaring, producing a mechanical interlock under flat-die conditions. The experimental tests, performed by applying a 25 ton pressing force to the joint, exhibited the same deformation sequence, confirming that the model captures the governing mechanisms and reproduces the distinct response observed for the standard and reversed orientations. In addition, simulations evaluated with the normalized Latham–Cockcroft criterion indicate damage localization at the perimeter of the flared rivet stem. Consistently, experiments revealed radial cracks initiating at the same location, while no fractures were observed in the sheet material, as predicted. The only additional cracking observed in the specimens occurred in the paint coating of the painted EoL samples, which showed superficial coating cracks without substrate failure.

Conclusion

This study demonstrated the feasibility of a rivet-based joining-by-forming process specifically designed for flat-die operation, enabling direct integration into EoL sheet-metal flattening workflows. Numerical simulations highlighted the critical influence of rivet geometry on buckling and flange formation, leading to an optimized design capable of forming a stable mechanical interlock without dedicated dies. The proposed approach addresses the geometric variability and uncertain formability of reclaimed automotive sheets by eliminating the need for shaped dies and dedicated joining equipment.

Finite element simulations were used to analyse rivet deformation, flange formation, and damage evolution under axial compression. The results demonstrated that rivet geometry particularly stem length and chamfer configuration governs the buckling mode and the stability of outward flaring. The proposed rivet promoted controlled radial outward expansion of the stem, resulting in a stable mechanical interlock while limiting sheet deformation. Damage predictions based on the normalized Latham-Cockcroft Normalized Criterion indicated localized cracking at the flared rim of the rivet, without critical failure of the sheets or of the joint. Numerical push-out simulations on a joint composed of a rivet estimated a maximum load of approximately 2.5 kN.

Experimental tests confirmed the numerical simulations with the creation of a stable interlock in both orientations, with no structural damage on the sheets found. Fractures were confined to the pressed rivet stem border and the paint coating layer on samples that were painted. Tensile tests yielded average maximum load of 1.71 kN for single rivet configurations joining 0.99 mm thick samples and 2.675 kN for double rivet configurations joining 0.83 mm thick samples.

Overall, the results demonstrate that mechanically reliable joints can be achieved using exclusively flat dies, eliminating the need for shaped cavities or dedicated joining systems. The proposed process provides a low-tooling, low-energy solution suitable for circular manufacturing routes based on direct reuse of automotive sheet metal.

References

- [1] «International Energy Outlook 2016 With Projections to 2040», U.S. Energy Information Administration, mag. 2016. doi: <https://doi.org/10.2172/1296780>.
- [2] «European Steel in Figures - Covering 2023», Eurofer, 2024. <https://www.eurofer.eu/publications/brochures-booklets-and-factsheets/european-steel-in-figures-2024>.
- [3] F. E. K. Sato e T. Nakata, «Energy consumption analysis for vehicle production through a material flow approach», *Energies*, vol. 13, fasc. 9, mag. 2020, doi: 10.3390/en13092396.
- [4] D. Farioli, M. Fabrizio, E. Kaya, V. Mussi, e M. Strano, «Energy measurements and LCA of remanufactured automotive steel sheets», in *Materials Research Proceedings*, Association of American Publishers, 2023, pp. 1947–1956. doi: 10.21741/9781644902479-210.
- [5] A. K. Ali, Y. Wang, e J. L. Alvarado, «Facilitating industrial symbiosis to achieve circular economy using value-added by design: A case study in transforming the automobile industry sheet metal waste-flow into Voronoi facade systems», *Journal of Cleaner Production*, vol. 234, pp. 1033–1044, ott. 2019, doi: 10.1016/j.jclepro.2019.06.202.
- [6] G. Meschut et al., «Review on mechanical joining by plastic deformation», *Journal of Advanced Joining Processes*, vol. 5. Elsevier B.V., june 2022. doi: 10.1016/j.jajp.2022.100113.
- [7] J. Wu, C. Chen, Y. Ouyang, D. Qin, e H. Li, «Recent development of the novel riveting processes», doi: 10.1007/s00170-021-07689-w/Published.
- [8] T. Trzepieciński e S. M. Najm, «Current Trends in Metallic Materials for Body Panels and Structural Members Used in the Automotive Industry», *Materials*, vol. 17, no. 3, p. 590, jan. 2024, doi: 10.3390/ma17030590.